Categorical edge-based analyses of phylogenomic data reveal conflicting signals for difficult relationships in the avian tree

Ning Wang[1,2,3*], Edward L. Braun[4], Bin Liang[1,2], Joel Cracraft[3], Stephen A. Smith[2]

[1]College of Life Sciences, Inner Mongolia University, Hohhot, 010070, China

[2]Department of Ecology & Evolutionary Biology, University of Michigan, 1105 N University Ave, Ann Arbor, MI 48109-1048, USA

[3]Department of Ornithology, American Museum of Natural History, New York, NY 10024, USA

[4]Department of Biology, University of Florida, Gainesville, FL 32607, USA

***Correspondence**

Ning Wang

College of Life Sciences, Inner Mongolia University, Hohhot, 010070, China

Email: ningwang83@hotmail.com

ABSTRACT:

Phylogenetic analyses fail to yield a satisfactory resolution of some relationships in the tree of life even with genome-scale datasets, so the failure is unlikely to reflect limitations in the amount of data. Gene tree conflicts are particularly notable in studies focused on these contentious nodes, and taxon sampling, different analytical methods, and/or data type effects can further confound analyses. Although many efforts have been made to incorporate biological conflicts, few studies have curated individual genes for their efficiency in phylogenomic studies. Here, we conduct an edge-based analysis of Neoavian evolution, examining the phylogenetic efficacy of two recent phylogenomic bird datasets and three datatypes (ultraconserved elements [UCEs], introns, and coding regions). We assess the potential causes for biases in signal-resolution for three difficult nodes: the earliest divergence of Neoaves, the position of the enigmatic Hoatzin (*Opisthocomus hoazin*), and the position of owls (Strigiformes). We observed extensive conflict among genes for all data types and datasets even after meticulous curation. Edge-based analyses (EBA) increased congruence and provided information about the impact of data type, GC content variation (GC_{CV}), and outlier genes on each of nodes we examined. First, outlier gene signals appeared to drive different patterns of support for the relationships among the earliest diverging Neoaves. Second, the placement of Hoatzin was highly variable, although our EBA did reveal a previously unappreciated data type effect with an impact on its position. It also revealed that the resolution with the most support here was Hoatzin + shorebirds. Finally, GC_{CV}, rather than data type (i.e., coding vs non-coding) *per se*, was correlated with a signal that supports monophyly of owls + Accipitriformes (hawks, eagles, and New World vultures). Eliminating high GC_{CV} loci increased the signal for owls + mousebirds. Categorical EBA was able to reveal the nature of each edge and provide a way to highlight especially problematic branches that warrant a further examination. The current study increases our understanding about the contentious parts of the avian tree, which show even greater conflicts than appreciated previously.

keywords: edge-based analyses; Neoavian resolution; GC content variation; outlier signal

1. Introduction

The growth of genomic datasets is increasingly facilitating the resolution of phylogenetic relationships, although as datasets have grown, so has conflict. This may involve gene-tree discordances within a single study (e.g., Wang et al. 2019) or the resolution of difficult and controversial hypotheses found across multiple studies (e.g., Wickett et al. 2014; Puttick et al. 2018). Conflicting gene trees can be the result of biological processes such as hybridization, gene duplication and loss, and incomplete lineage sorting (ILS; see Table 1 for list of abbreviations) or they can be the result of artificial noise arising from, for example, assembly error, orthology inference, sequence alignment, model specification, and insufficient informative variation (Springer and Gatesy 2019). In part, due to these conflicts, several areas across the tree of life have consistently been difficult to resolve (Tarver et al. 2016; Shen et al. 2017) despite the use of genome-scale datasets (Foley et al. 2016) and increased taxa sampling (Prum et al. 2015; Wang et al. 2017) that benefit from growing effort and worldwide collaboration, as well as easier acquirement of ancient DNA (e.g., Chen et al. 2018).

Additionally, different analytical methods, and/or the inclusion or exclusion of multiple data types (Reddy et al. 2017) can result in conflicting resolutions, with issues regarding methodology (e.g., inaccurate evolutionary models) may be more difficult to address. In particular, difficult-to-resolve edges may be the result of low signal within very short internodes. Concatenation can overcome low signal by combining the signal from multiple genes but also assumes that all genes share a single evolutionary history, yet population genetic and molecular evolutionary processes can result in highly heterogeneous gene trees and violate this assumption (Kolaczkowski and Thornton 2004; Kubatko and Degnan 2007; Edwards 2009). The most commonly used summary coalescent methods (e.g., ASTRAL III, Zhang et al. 2018; MP-EST, Liu et al. 2010), on the other hand, accommodate gene tree conflicts but assume accurately estimated gene trees for neutrally evolving gene regions that are free of intralocus recombination and only exhibit conflict due to ILS (Springer and Gatesy 2016). However, typical phylogenomic datasets include many genes that violate at least some of these assumptions (although the methods may be robust to these model violation). Also, when analyzing large genomic datasets, many genes will have experienced episodic periods of strong selection, or linkage and hitchhiking can also cause violation of neutral evolution for most genomic regions (e.g., Wang et

al. 2021). Moreover, some genes show within-gene conflict, supporting multiple trees (Kimball et al. 2013; Mendes et al. 2019). These observations highlight the importance of examining individual genes in phylogenetic analyses, especially when errors in alignment, assembly, and gene-tree estimation may be common as dataset size increases and larger datasets are more difficult to curate (Gatesy and Springer 2017; Liu et al. 2017).

With ~10,500 living species, birds represent the most species-rich group of tetrapod vertebrates. Despite their importance, several controversial relationships in Neoaves have not been settled (e.g., Reddy et al. 2017). Challenges to resolving these nodes are not unexpected considering that neoavian birds likely experienced a very rapid radiation (e.g., Ericson et al. 2006; Jarvis et al. 2014; Prum et al. 2015; Houde et al. 2020). Although genome-scale datasets have facilitated the recovery of many relationships (e.g., passerines + parrots, flamingos + grebes, sunbittern + tropicbirds, and core landbirds; Hackett et al. 2008; Wang et al. 2012; McCormack et al. 2013; Jarvis et al. 2014; Suh et al. 2015; Braun et al. 2019; Sangster et al. 2022), the Neoaves are still well-known for multiple, extremely recalcitrant nodes. Specifically, the earliest divergences of Neoaves remain one of the most difficult phylogenetic problems in vertebrates, which has even been suggested to represent a hard polytomy (Suh 2016, but see Reddy et al. 2017). Within Neoaves, the positions of Hoatzin (*Ophisthocomus hoazin*) and owls (Strigiformes) remain especially problematic as well as being significant for the analysis of avian development, life history, and morphological traits. The Hoatzin is a bizarre and enigmatic bird species. It converts plant cellulose to simple sugars using microbial foregut fermentation (Domínguez-Bello et al. 1994) and has a modified skeleton (sternum) to accommodate a large crop. Also, Hoatzin chicks have claws on two of their wing digits (Hughes and Baker 1999). The unique features of the Hoatzin have confounded efforts to understand its phylogenetic position for decades, leading to the placement of Hoatzin with diverse taxa such as landfowl (Galliformes), cuckoos (Cuculiformes), or turacos (Musophagiformes) (Hughes and Baker 1999). Owls are nocturnal predators with raptorial features, but their relationships have been obscure. Within Neoaves there are at least two distinct raptorial lineages. The first is the falcons (Falconiformes *sensu stricto*), which have now been shown to be related to parrots and passerines, whereas the second, Accipitriformes, includes the hawks, eagles, and vultures. Presently, it remains unclear whether owls represent a third raptorial lineage or whether they are sister to hawks, eagles, and vultures. This uncertainty impacts our understanding of the evolution of raptorial features.

107 Recent avian studies have suggested that phylogenetic reconstruction is biased by the
108 source of the data (e.g., exon, intron, or UCE [ultraconserved element], Reddy et al. 2017),
109 which we refer to as data type effects. For example, in Jarvis et al. (2014), concatenated analyses
110 of exons, introns, and UCEs were largely discordant among each other. The resolution of owls
111 and the topology for the earliest split of Neoaves have been shown to vary among different data
112 types (Reddy et al. 2017; Braun et al. 2019; Braun and Kimball 2021). In contrast, the position of
113 the Hoatzin has been even more variable across studies (e.g., Reddy et al. 2017) and its position
114 does not exhibit an obvious correlation with data type. Due to biased base composition and high
115 GC content variation (hereafter GC_{CV}), exons received the most criticism for model violation and
116 impact on phylogenetic reconstruction (Jarvis et al. 2014; Reddy et al. 2017; Braun and Kimball
117 2021). Using models that incorporate base compositional heterogeneity (e.g., Galtier and Gouy
118 1998; Morgan et al. 2013) might improve analyses, but dramatic incongruence among gene trees
119 is often observed within data types (e.g., Jarvis et al. 2014) so the available models that
120 incorporate base compositional heterogeneity are unlikely to eliminate incongruence among
121 exonic trees. Nevertheless, finding that exons are generally misleading in the relationships they
122 reconstruct would have far reaching implications for phylogenomic analyses as transcriptomic
123 and targeted sequencing data have become more common (e.g., Prum et al. 2015; Wang et al.
124 2019).
125 Herein we examine conflicting signals within two major avian datasets: Jarvis et al. (2014)
126 and Prum et al. (2015). We conduct constrained phylogenetic analyses (edge-based analyses
127 [EBA], see Smith et al. 2020) to examine the relative support for alternative resolutions of three
128 relationships within Neoaves that have proven to be difficult to resolve; specifically, we examine
129 the earliest divergence within Neoaves, the position of Hoatzin, and the position of owls. We
130 explore the efficacy of large datasets to resolving these relationships by carefully curating
131 individual genes and assessing their contribution to the support for alternative hypotheses. In
132 addition to individual gene evaluations, we focus on dissecting the phylogenetic signal
133 associated with different data types (exon, intron, and UCE) and examine other factors, such as
134 GC_{CV} (Foster and Hickey 1999) and gene evolutionary rate (Chojnowski et al. 2008) that might
135 also influence phylogenetic estimation. The inclusion of multiple data types facilitates
136 examination of whether phylogenetic signal from protein-coding regions were different from

137 those of non-coding regions. Through these analyses, we seek to better characterize the ability of
138 large datasets to address difficult phylogenetic questions in birds and other groups.
139

140 **2. Materials and Methods**

141 We have illustrated the data sources and overall analytical framework for this study using the
142 flow chart in Fig. 1.

143

144 ***2.1 Data acquisition and filtering***

145 We obtained 8251 exons, 2516 introns, and 3769 UCEs from Jarvis et al. (2015) (hereafter Jarvis
146 data). To increase the phylogenetic signal from individual genes and eliminate potential
147 systematic error or noise, we conducted several filtering steps. First, genes having a short
148 alignment (< 500bp) and/or missing taxa (< 42 species after deleting sequences with > 70% gaps
149 in the alignment) were excluded. Second, we reconstructed ML gene trees using IQTREE (v.
150 1.6.3, Nguyen et al. 2014) with the GTR + Γ model and 1000 Ultra-Fast Bootstrap (UFBS, Minh
151 et al. 2013) replicates. Trees having outgroups that clustered within ingroups (i.e., non-bird
152 species nested within birds, and/or species from Palaeognathae and Galloanserae nested within
153 Neoaves) were treated as systematic error and excluded from additional analyses. Finally, trees
154 with extremely long branch lengths (> 1 expected substitution per site) were also excluded due to
155 potential error in ortholog identification. Scripts are available at
156 https://bitbucket.org/ningwang83/avian_conflict_assess. In addition, the original 259 sequence
157 alignments and gene trees from Prum et al. (2015) were downloaded and filtered following a
158 same procedure (hereafter Prum data).
159

160 ***2.2 Examination of gene tree resolution diversity***

161 In general, we focused on three controversial edges on the avian tree of life: the earliest
162 divergence in Neoaves and those encompassing the positions of the Hoatzin and owls (Table 2).
163 We assessed the diversity of resolutions in the gene trees as follows. First, we examined the
164 topological distributions of ML gene trees (Fig. 2) in relation to the three focal edges under
165 different support cutoffs (i.e., ≥ 0%, 50%, 70%, 95% support based on either BS [bootstrap] or
166 UFBS, Hoang et al. 2018). Second, we examined Robinson–Foulds (RF, Robinson and Foulds
167 1981) distances among gene-trees for each data type, as well as between each gene tree and the

concatenated TENT_ExaML species tree from Jarvis et al. (2014) and the concatenated RAxML tree from Prum et al. (2015). RF distances were calculated using the *bp* script (https://github.com/FePhyFoFum/gophy), which allows non-overlapping taxa in the gene trees. Finally, to quantify the relative strength of the phylogenetic signal for a certain edge, we calculated the ICA values (Internode Certainty All; Salichos et al. 2014; see Table 1) on the species trees (same as above) from the filtered gene trees of each data type respectively. These analyses were conducted using RAxML 8.2.11 (Stamatakis 2014) with the GTRCAT model and lossless support to accommodate partial gene trees (Kobert et al. 2016).

2.3 Edge-based analyses – Assessment for constraint topologies for three focal edges

We selected several alternative topologies from previous large-scale studies (Table 2) for each of the three focal edges. For the Jarvis data, gene trees were reconstructed in IQTREE using one constrained edge at a time and optimizing the remainder of the tree. This analysis was conducted for each locus and every focal edge (Fig. 3). Since the ML gene trees typically exhibited topologies different from published dominant relationships (see discussion bellow), genes were excluded if their ML gene tree was incompatible with any testing constraint under a 95% UFBS cutoff (i.e., any locus with an ML gene tree that has a focal node conflict with all test hypotheses would be kept only if the conflicting node was weakly supported [< 95% UFBS]). To identify the best hypothesis, we conducted the following analysis:

(1) We compared ln$L$ (log likelihood) scores among conflicting alternative topologies for a single edge for each gene and identified its supporting (i.e., the best) topology.
(2) We calculated the difference in ln$L$ (Δln$L$) between the best and the second-best resolutions for each gene. At this stage, we also identified potential outlier genes (cases where Δln$L$ fell out of the smooth distribution among other genes) by eye.
(3) We summed Δln$L$ for each constraint from supporting or significantly supporting (Δln$L > 2$) genes (referred to as $\sum\Delta$ln$L$ or $\sum$sigΔln$L$).
(4) We identified the overall best topology either supported or significantly supported (Δln$L > 2$) using two criteria: the largest number of genes ($\sum$Ng: simply the number of genes supporting a specific topology) and the highest $\sum\Delta$ln$L$ (or $\sum$sigΔln$L$) scores (Fig. 3).

198 Genes for which the ln*L* could not be calculated given specific constraint topologies (this occurs
199 when relevant taxa are missing) were excluded from the calculation.
200 We manually examined the outlier genes for misalignment and collected information
201 about the functions of them. We did this because positive selection can give rise to convergent
202 evolution, at least in principle, and genes with a specific function might group corresponding
203 species together and mislead phylogenetic inferences. For example, the hearing gene *Prestin*
204 grouped echolocating taxa (microbats and toothed whales), presumably reflecting convergence
205 (Li et al. 2010). Using BLAST, we determined outlier exons whether their function might be
206 related to the outlier topology. However, we did not conduct lineage-specific selection analyses
207 for outlier exons as their alignments contained several premature stop codons.
208 To control for the impact of taxon sampling on topological preference, we also conducted
209 EBA using genes from the large sampling (i.e., 198 bird species) of Prum et al. (2015), following
210 similar processes and criteria indicated above. To limit CPU time, the RAxML 8.2.11
211 (Stamatakis 2014) with GTRCAT model was used. The ML gene-trees including BS support
212 built with RAxML were directly retrieved from Prum et al. (2015). We also reduced the number
213 of constraint topologies to include only three hypotheses for each focal edge (see Results and
214 Discussion 3.3). Results were organized after filtering out loci with gene-tree incompatibilities
215 with any testing constraints under 70% BS cutoff (Hillis and Bull 1993). In addition, to examine
216 the sampling effect on the hypotheses examined here, we focused on the earliest diverging
217 Neoaves and assessed five additional hypotheses by referring one single lineage (i.e.,
218 caprimulgiforms [nightjars], Hoatzin, charadriiforms [represented by plovers], gruiforms
219 [cranes], or cuculiforms [cuckoos], Fig. 4) as sister to other Neoaves and conducted EBA with
220 Jarvis data using the same criteria mentioned above.
221 In order to assess influence of GC_{CV} and tree length (i.e., gene evolutionary rate) on tree
222 reconstruction using different data types, we sorted the filtered genes from Jarvis et al. (2014)
223 based on their GC_{CV} and tree length. We characterized GC_{CV} using a method similar to Reddy et
224 al. (2017). We excluded the crocodilian outgroups and calculated the GC content for sites that
225 are variable within birds. Then we calculated three different ΔGC metrics (ΔGC_{50}, ΔGC_{90}, and
226 ΔGC_{100}), which represent the GC content difference between a high-GC and a low-GC taxon.
227 The three different metrics differ in the high- and low-GC taxa that we selected; for ΔGC_{50} it was
228 the upper and lower quartile, for ΔGC_{90} it was the 95th and 5th percentile, and for ΔGC_{100} it was

229 the maximum and minimum. We ordered genes based on ΔGC_{90} to balance the GC difference
230 and similarity among data types (i.e., maximize differences while eliminating outlier signals, Fig.
231 5A) and examined the gene trees in the upper (i.e., high GC_{CV}) and lower (i.e., low GC_{CV})
232 quartiles of the variation for their supporting pattern to each testing edge (Fig. 5B). We
233 conducted similar analyses by sorting genes based on their total tree length and compared
234 support for focal edges between gene sets from the upper and lower quartile of the tree lengths
235 (Fig. 5C and D).
236
237 ***2.4 Comparison of tree topologies within genetic regions***
238 Within-genetic region comparisons were conducted using exons and UCEs from Jarvis et al.
239 (2014), which have high alignment quality without long indels, in addition to the Prum dataset.
240 We split the genes into 1000bp chunks, omitting the short leftovers. We conducted ML analyses
241 in IQTREE based on GTR + Γ model with uncertainty measured using both SH-aLRT and UFBS,
242 each with 1000 replicates. Edges with < 80% SH-aLRT or < 95% UFBS support were collapsed.
243 We note that this requirement is extremely conservative but limits false positives. We also re-
244 estimated gene trees using these same criteria for consistency among these tests. We then
245 compared trees from gene region fragments to the ML gene trees based on the entire gene region
246 and noted conflicts.
247
248 ***2.5 Coalescent simulation – assessing the performance of EBA for deep coalescence***
249 We conducted simulations to assess the performance of EBA in recovering the potential true
250 topology at edges under differing level of ILS. The Jarvis et al. (2014) MP-EST* TENT tree,
251 which was built with a binned MP-EST* method (Mirarab et al. 2014), was used as the *model*
252 *species tree*. We rescaled the terminal branch length of the model species tree to make it
253 ultrametric and generated 500 simulated gene trees using the neutral coalescent model with the
254 *treesim.contained coalescent_tree* module in Dendropy 4.2.0 (Sukumaran and Holder 2010). We
255 rescaled the internal branches of these gene trees with 0.01, which is estimated by comparing the
256 coalescent and substitution branch lengths (BLs) in the empirical data of Jarvis et al. (2014).
257 Duchêne et al. (2018) found that the tip branch-lengths (tipBLs) are best to be proportional
258 among species across gene trees. Thus, we first obtained the distribution of BLs for each species
259 from the empirical ML gene trees of Jarvis et al. (2014). Then, we generated tipBLs for each

simulated gene by selecting the same percentile tipBLs value from the empirical distribution of each species. This rescaling method ensures a proportional tipBLs across all gene trees. To simulate different types of data, we estimated the branch length distributions, and the modeling parameters (see below) from exons, introns and UCEs, respectively. Here for each datatype, we built a coalescent species tree with ASTRAL III (Zhang et al. 2018) using these rescaled simulated gene trees. Moreover, the average RF distance (ARFD) between the model species tree and the simulated gene trees was used to reflect the level of overall ILS.

We generated one sequence alignment with length of 800-3000bp for each simulated gene tree using Seq-Gen (Rambaut and Grass 1997, implemented in Dendropy). All alignments were generated using the GTR + Γ model with model parameters (base composition, α parameter for Γ distribution, and GTR substitution rates) selected randomly from the density distribution of the Jarvis data of exons, introns, and UCEs, respectively. Simulations were repeated once for each data type to validate results, so there were six sets of 500 simulated alignments in total. Then we obtained *ML estimates of simulated gene trees* for these simulated alignments in IQTREE using the GTR + Γ model. In addition, 184 bipartition constraints were generated from 27 species-tree estimates constructed by Jarivs et al. (2014), which provide a reasonable representation of the extent variation of species tree hypotheses as to bird relationships, so that all the bipartitions in the model species tree were included. The EBA were conducted using the simulated alignments following the method described above on the three difficult focal edges that exhibit higher level of ILS as well as some commonly accepted edges that exhibit lower levels of ILS, including **I**, **II**, **III**, and **V** (Table 1) from the "magnificent seven" superordinal groups (Reddy et al. 2017). We also conducted ASTRAL analyses using the ML estimates of simulated gene trees. We calculated the mean gene-tree estimation error (GTEE) by using Dendropy to calculate the unweighted RF distance between the simulated gene trees and the ML estimates of the simulated gene trees, which we averaged across all genes. To compare the performance of concatenation analyses, we concatenated the simulated alignments of each data type and conducted ML analyses in RAxML 8.2.11 using GTR + Γ model, partitioned by locus, and we calculated node support using 200 bootstrap replicates.

3. Results and Discussion

3.1 Gene informativeness

291 After careful data curation, we obtained 5062 exons, 1409 introns and 3370 UCEs (Table S1)
292 from Jarvis et al. (2015). All data from Prum et al. (2015) passed the filtering processes and were
293 therefore retained.
294 We examined the extent to which each genomic partition had information to resolve
295 nodes within the tree. We found that each gene in the Jarvis dataset supported, on average, 24 (≥
296 70% UFBS) or 15 (≥ 95% UFBS) of the 47 internal nodes, respectively, whereas the Prum data
297 supported (≥ 70% BS) ~110 out of 197 internal nodes on each gene tree, with a maximum of 144
298 and minimum of 22 (Fig. 2A). The low support on many nodes is likely caused by the relatively
299 low phylogenetic signal for individual genes that are subject to high GTEE (Molloy and Warnow
300 2018), especially across such broad relationships. Although introns generally supported more
301 relationships, the number of supporting nodes appeared to correspond to alignment length (Fig.
302 S1). For the three edges of interest, only 23%– 33% exons, 38%–51% introns, and 34%–43%
303 UCEs in the Jarvis data obtained ≥ 70% UFBS on ML gene trees after excluding genes with
304 missing owls or Hoatzin. In the Prum data, similarly, only four loci obtained supports (>70% BS)
305 on their ML gene trees for the resolution of Hoatzin, two genes showed supports for the earliest
306 diverging clade of Neoaves, whereas no gene supported the position of owls. 113 genes even
307 showed non-monophyly of owls (i.e., the two families of owl had distinct positions in the tree) in
308 Prum et al. (2015). These results suggest that most loci have limited information for resolving
309 the contentious edges and therefore a high potential for GTEE from these genome data,
310 regardless of the sources of conflict.
311
312 ***3.2 Diversity of resolutions***
313 Many gene regions across datasets and datatypes did not demonstrate a strong preference for any
314 specific resolution regarding the three focal relationships (Fig. S2). However, to ascertain the
315 nature of the support for alternative resolutions when support was indicated, we firstly examined
316 how many different resolutions were supported by different genes. We observed, for example in
317 the Jarvis exons, there were more than 1500 alternative resolutions for each focal relationship.
318 Most of these were unsupported (~ five resolutions obtained ≥ 95% UFBS and ~40 resolutions
319 obtained ≥ 50% UFBS) or were present in fewer than 10 gene trees (i.e., rare resolutions, Fig.
320 2B). Even the best-supported topology for each data type was still present in less than 5% of
321 gene trees. The situation was similar for introns and UCEs (Fig. S3A). The Prum data had 259

322 loci, and we identified 110 or more topologies for each focal edge, but only 3 – 16 topologies
323 had > 50% BS, within which more than 80% were found in a single gene (Fig. S3B).
324 To properly discuss the uncertainty of the focal relationships and the large number of
325 plausible topological alternatives, we have adopted a compact notation for clades. For example,
326 the root of Neoaves in the Jarvis et al. (2014) TENT_ExaML is between **VI** + **VII** (Table 1) and
327 all other Neoaves. Hereafter, we refer to this topology as **VI**+**VII** sister, and both the **VI**+**VII**
328 clade and the remaining Neoaves (i.e., the edge that supports the **VI**+**VII** sister relationship)
329 have 100% BS in the TENT_ExaML and the binned MP-EST* trees in Jarvis et al. (2014).
330 Houde et al. (2019) conducted additional analyses of the Jarvis non-coding (intron and UCE)
331 data, using both nucleotide sequences and indels, and they also reported the same basal topology
332 (albeit with local posterior probabilities <1.0). However, the **VI**+**VII** sister obtained -0.051
333 (intron), -0.272 (UCE), and -0.317 (exon) ICA values in our analyses, indicating substantial
334 conflicting signals among gene trees, and a better supported alternative conflicting relationship
335 as shown in the ML topology distribution (Fig. S3). The very different ICA values are also
336 indicative of a data type effect, with introns showing a very different signal than UCEs or exons.
337 Similar situations were also found for the other two focal edges (i.e., for the Hoatzin and owls)
338 and in both datasets (not shown).
339 The diversity of resolutions can also be observed by the RF distances among gene trees.
340 Trees based on Jarvis exons and UCEs exhibited more among-gene tree differences (~65, 69% of
341 the edges, Fig. S4) than do trees based on introns (~58, 62% of the edges), implying the potential
342 of high GTEE in these gene trees (Simmons et al. 2016). Similar patterns were also found when
343 comparing gene trees to the species-tree topologies. The RF distances among gene trees for the
344 Prum data were usually larger than 150 (38% of the edges) and as high as 300 (76% of the edges,
345 Fig. S4), suggesting high topological diversity that may be a reflection of dense taxon sampling
346 in the data.
347
348 ***3.3 Edge-based analyses (EBA)***
349 Examining conflicting signals in large-scale datasets is perhaps the foremost challenge in
350 systematics as we have entered the phylogenomic era. One common analytical framework is
351 concatenation, which is known to be a useful methodology in many contexts (Bryant and Hahn
352 2020) despite its failure to model the multispecies coalescent (Edwards et al. 2016). However,

353 the utility of concatenation for the examination of conflict is limited because they generally yield
354 a single tree. Low support values in concatenated analyses can either provide evidence of
355 conflict or it could reflect the absence of any signal in the data. Fundamentally, there are only
356 two ways to examine conflict using the concatenated approach. First, one can subdivide data
357 based on some criterion, such as coding vs. non-coding data (e.g., Jarvis et al. 2014, Reddy et al.
358 2017; Braun and Kimball 2021) or protein structure (e.g., Pandey and Braun 2020; Gordon et al.
359 2021), and conduct concatenated tree searches on the data subsets. Second, one can examine
360 differences in the tree selection criterion (typically the likelihood) for various topologies at the
361 level of the genes (Shen et al. 2017) or the individual site level (Kimball et al. 2013). Both
362 approaches have limitations: the former only allows assessment of data type effects whereas the
363 latter can only yield information about a small number of topologies due to computational time
364 limit.

365 An alternative way to examine conflicts involves comparisons of gene trees that can have
366 any topology. However, analyses of individual genes are subject to high GTEE, so many
367 bipartitions in estimated gene trees may be spurious. Moreover, there can be conflicts within
368 gene regions due to intralocus recombination and other factors (see section 3.5). Ultimately, it is
369 difficult to determine whether the extensive conflict among estimated gene trees reflects a
370 mixture of meaningful biological signals or simply random resolutions due to GTEE. Our EBA
371 of genes lie between concatenation and simple gene-tree analysis. This approach limits the
372 consideration of gene-tree topologies to those containing a specific bipartition. In this study, we
373 have limited the testing bipartitions to those commonly identified previously (see Table 2) or
374 those present in large numbers of gene trees. Comparison of the results given the two
375 complementary criteria, $\sum\Delta\ln L$ and $\sum$Ng, can also provide evidence for outlier genes; when
376 $\sum\Delta\ln L$ for a specific edge is much larger than $\sum$Ng, it might imply that a relatively small number
377 of genes are contributing a large amount of the $\ln L$ differences among alternative resolutions.
378 Overall, this edge-based approach should limit GTEE while still retaining the advantages of gene
379 tree-based analyses and provide information about conflicting signals (see also discussion in
380 Mount and Brown 2022).

381 We examined gene-wide support for the dominant alternative resolutions of the three
382 focal edges that have been previously published (Table 2). After excluding loci with strong

383 incompatible node to our test hypotheses, we obtained 4194 – 5019 exons, 1134 – 1274 introns,
384 and 3165 – 3295 UCEs for each focal relationship (Table S1) from the filtered Jarvis data.
385 Regarding the earliest diverging Neoaves (Fig. 4A and Table 2), all data types had the
386 highest support for placing doves sister to all other Neoaves (Fig. S2) when five published
387 hypotheses were tested. When we expanded the set of hypotheses to include the most prevalent
388 topologies in the gene trees (Fig. 4A, hypotheses 6–10), support was more evenly distributed
389 across them (Fig. 4A). For the other two edges, Hoatzin were sister to shorebirds (*S*), and owls
390 were sister to mousebirds (*M*, Fig. 4B and C). These findings obtained support, although few, in
391 previous studies, including owls + *M* in a reanalysis of shallow-filtered Jarvis UCE data (Gilbert
392 et al. 2018), doves sister to all other Neoaves in the UCE indel tree (Houde et al. 2019), and
393 Hoatzin + *S* in the complete UCE data matrix (McCormack et al. 2013). Moreover, the
394 relationships published in the Jarvis et al. (2014) TENT tree (i.e., **VI+VII** as earliest Neoaves,
395 *S*+*CR* sister to Hoatzin, and *M* + *W* sister to owls) were only weakly supported (Fig. 4).
396 To examine taxon sampling effect in EBA, we obtained up to 258 loci (Table S2) from
397 Prum et al. (2015) after excluding strong incompatible loci. We tested three constraints for each
398 focal edge, with one constraint directly retrieved from Prum et al. (2015) tree and two from the
399 top two published hypotheses supported by the Jarvis data (i.e., **V/VII**/doves as earliest Neoavian
400 branch, **I**/*S*/**V** sister to Hoatzin, and [*M*+*W*]/*M*/*EHV* sister to owls). The best relationships
401 supported by the Prum data were the same as found in the Jarvis data (e.g., Hoatzin + *S*; owls +
402 *M*, Table S2), indicating a limited taxon-sampling effect on EBA, which increase congruence
403 between analyses of the Prum and Jarvis data. Moreover, analyses focused on the earliest
404 diverging Neoaves using the Prum data revealed a major impact of genes with a large $\Delta\ln L$. For
405 example, we noted that gene L111 encoding an FH2 domain containing 1 protein (FHDC1,
406 whose homolog may play a role in both cell shape and microtubule polymerization in humans),
407 disproportionately contributed 171 $\Delta\ln L$ to support **VII** as the earliest divergence of Neoaves.
408 We did not detect alignment error or lineage specific positive selection for this gene. Moreover,
409 eliminating FHDC1 would not shift the best supported hypothesis given the $\sum\Delta\ln L$ criterion
410 (Table S2). Regardless of the details, the best-supported hypothesis in these EBA of the Prum
411 data were never the relationships present in the Prum et al. (2015) tree; they were hypotheses
412 found in EBA of the Jarvis data.
413

414 ***3.4 Complex data type effects revealed by categorical edge-based analyses***

415 The relatively even distribution of support for various hypotheses regarding the earliest diverging
416 Neoaves when we examined 10 alternatives (Fig. 4A) suggests a very high degree of conflict
417 among gene trees. However, this result also suggests a hypothesis-sampling-effect (i.e., the more
418 hypotheses tested, the more widely distributed the support). It further provides evidence for a
419 data type effect on best hypotheses: exons supported cuckoos sister, introns continued to support
420 doves sister, and UCEs supported either clade **VII** (largest $\sum\Delta\ln L$) or cuckoos (largest $\sum$Ng). It
421 is noteworthy that Jarvis et al. (2014) placed **VII** sister to all other Neoaves in their concatenated
422 analysis of UCEs, and the $\sum\Delta\ln L$ criterion is similar to the criterion used for tree selection in ML
423 analyses. However, the observation that UCEs placed **VII** sister in fifth place based on the
424 alternative criterion – $\sum$Ng, suggests that the support for **VII** sister reflects a limited number of
425 UCE loci with large $\Delta\ln L$ values (Fig. 4A, Table S3). However, the functions of many UCEs are
426 unclear and it is difficult to examine selection on non-coding loci, so we did not attempt to
427 determine whether there might be a functional basis for the outlier UCEs. There were other
428 differences among data types in the rank order of suboptimal hypotheses. For example, when the
429 $\sum\Delta\ln L$ criterion is used, **VI + VII** as the earliest Neoavian branch received much higher support
430 in analyses of non-coding data, especially introns, than it did in analyses of coding data (10.9%
431 for introns, 7.4% for UCEs, and 2% for exons). These results agree with the data type effects
432 reported by Reddy et al. (2017) and by Braun and Kimball (2021), although the differences
433 among data types also appear to be more complex than the results suggested before.

434 Reddy et al. (2017) pointed out that data type had a major impact on the topology for the
435 deepest divergence in Neoaves, with analyses of coding data supporting a **V** sister topology and
436 analyses of non-coding data supporting either **VI+VII** sister (introns) or **VII** sister (UCEs).
437 Several studies (Jarvis et al. 2014; Reddy et al. 2017; Braun and Kimball 2021) pointed out that
438 avian coding data typically exhibit greater GC_{CV} than do non-coding data. Previous studies (e.g.,
439 Jermiin et al. 2004; Duchêne et al. 2017) have demonstrated that high GC_{CV}, when fit to a
440 homogeneous model, can results in biased phylogenetic estimation. Applying models with more
441 heterogeneous assumptions (e.g., Galtier and Gouy 1998; Holland et al. 2013) has the potential
442 to improve estimates of phylogeny, although the available programs that implement these models
443 are challenging to apply to phylogenomic datasets (see additions discussion in Reddy et al. 2017).
444 Since our EBA provide a sensitive tool to examine conflicting signals in phylogenomic datasets

445 we assessed the impact of GC_{CV} in the Jarvis et al. (2014) data on the conflicts among data types
446 that we observed.
447 Generally, ΔGC_{50} was similar among data types but ΔGC_{90} and ΔGC_{100} variation was
448 larger for exons than for introns and UCEs, consistent with findings in Reddy et al. (2017) (Fig.
449 5A). After sorting genes based on ΔGC_{90}, about 1266 exons (E), 352 introns (I) and 842 UCEs
450 (U) were retained in the upper (H) or lower (L) quartile category. If GC_{CV} has an impact on
451 inference we would expect different patterns of support between GC_{CV} categories within the
452 same data type. Indeed, owls + *EHV* showed much higher support (both ∑Ng and ∑Δln*L*) in all
453 high GC_{CV} makers (Figs. 5B and S5), and such signal is strongest in EH and IH (i.e., the high
454 GC_{CV} exons and introns). It seems the characteristics of high GC_{CV} genes tend to correlate with
455 owls + *EHV*. Braun et al. (2019) suggested that the position of owls in concatenated analyses was
456 subject to a data type effect, with analyses of coding data tending to yield the owls + *EHV*
457 topology. We found that support for owls + *EHV* was similar for the EL, IL, and UL datasets
458 (low GC_{CV} exons, introns, and UCEs, respectively) but much higher in the EH, IH, and UH (the
459 high GC_{CV} datasets). However, the signal for owls + *EHV* was still stronger in the high GC_{CV}
460 exons than in the high GC_{CV} introns and UCEs. Thus, our results imply that an interaction
461 between higher GC_{CV} and data type – not coding vs non-coding data type *per se* – is correlated
462 with the owls + *EHV* signal.
463 As previously noted, the position of Hoatzin has been highly variable across studies and
464 data type effects have not been noticed before (reviewed by Braun et al. 2019). The dominant
465 signal in our categorical EBA was Hoatzin + *S*, which is also present in the Jarvis exon c123 tree
466 and the McCormack et al. (2013) UCE tree. In the categorical EBA, there was higher support for
467 Hoatzin + *S* in high GC_{CV} markers (compare EH vs EL, IH vs IL, and UH vs UL; Fig. 5B), but
468 the support differences are quite trivial. In fact, support for alternative relationships of the
469 Hoatzin show more variations among data types (Figs. 5B and S5) regardless of GC_{CV} and tree
470 length. The most notable difference was a weaker support for Hoatzin + *S* and a stronger support
471 for Hoatzin + **V** in the introns (Fig. 5B and D). Provocatively, Hoatzin + **V** is present in the
472 Jarvis intron tree (albeit with only 70% BS) but it is not in the Jarvis UCE tree (which included
473 Hoatzin + *S* + *CR*, like the Jarvis TENT). These results are not consistent with a simple coding
474 vs noncoding effect for two reasons. First, the signal for Hoatzin + *S* is very similar in exons and
475 UCEs (Fig. 5B) but the Hoatzin + **V** was elevated in both noncoding data types. Second, Hoatzin

476 + **I**, which is found by Prum et al. (2015) using mostly coding data, received higher support in
477 introns and UCEs (Figs. 5B and S5) than it did in the Jarvis exons (Fig. 5). Thus, in agreement
478 with many previous studies, we find that the position of the Hoatzin is very difficult to resolve.
479 However, our EBA revealed a previously unappreciated and relatively complex data type effect
480 and further showed that Hoatzin + *S* was the strongest signal in all three data types.
481 The most prominent data type effect hypothesized by Reddy et al. (2017) was the **VI +**
482 **VII** sister to all other Neoaves (their non-coding topology) and **V** sister to all other Neoaves
483 (their coding hypothesis). Using our categorical EBA, **V** as sister to all other Neoaves did not
484 appear to have better support in exons than in introns or UCEs (Figs. 5B and S5). The data subset
485 with the highest support for **V** as the earliest neoavian branch was the high GC_{CV} UCEs (UH in
486 Fig. 5B). This support for **V** sister appears to result from one outlier gene (chr1_28895_s) that
487 contributes almost 40% of the $\sum\Delta\ln L$ (Table S3) for this relationship. Unsurprisingly, the total
488 number of genes ($\sum$Ng) that support **V** did not vary much among GC_{CV} categories or data types
489 (Fig. S5). As described above, **VI+VII** did appear to be better supported in introns and UCEs,
490 especially in the data subsets with high GC_{CV} and high tree lengths (i.e., IH and UH, Fig. 5B and
491 D). However, the number of genes ($\sum$Ng) supporting **VI+VII** did not vary much among
492 categories and data types (Fig. S5). Thus, the higher support for **VI+VII** sister appears to reflect
493 a relatively small number of genes that make high $\Delta\ln L$ contributions; given the much higher
494 proportion of signal for **VI+VII** sister in the IH and UH subsets (Fig. 5B), these genes with a
495 high $\Delta\ln L$ contribution must be especially common in the high GC_{CV} data subsets.
496 Evolutionary rate is another major factor in phylogenetic resolution (Chojnowski et al.
497 2008). Tree length (sum of branch lengths) variation suggests different overall rates of evolution
498 and different data types exhibited different patterns, with introns having larger tree
499 length/internode lengths and less variation than UCEs and exons (Fig. 5C). Tree length in these
500 datasets is primarily the result of tip lengths (Fig. 5C) as a consequence of sampling at high
501 taxonomic levels. In general, tree lengths did not have an obvious impact on support for different
502 hypotheses for each focal edge. However, we noticed two interesting patterns with respect to the
503 earliest diverging Neoaves (Fig. 5D). First, **VI+VII** as sister to all other Neoaves usually
504 received higher support in categories with high GC_{CV} and high tree lengths, but we noted that
505 **VI+VII** also received high support (i.e., the best) in the intron subset of low tree lengths (IL, Fig.
506 5D). Within this category, we identified one gene (e.g., 11117.intron, Table S3) contributing ~21%

507 of the ∑Δln*L* supporting this relationship. We did not detect any alignment issue in this gene and
508 its tree length is around the upper edge of this quartile set. Thus, its outlier signal may be driven
509 by some biological characteristics that may not be directly related to evolutionary rate. Second,
510 **VII** as sister to all other Neoaves received the highest support from the UCE subset of high tree
511 length (UH, Fig. 5D), consistent with the Jarvis et al. (2014) UCE tree. Again, an outlier gene
512 (chr8_1881_s, that contributed 1/3 ∑Δln*L*, Table S3) was identified, and its support for **VII** as
513 sister may be driven by certain characteristics that may or may not be directly related to its high
514 tree length.
515 As found previously, genes that have disproportionally high support for specific
516 relationships (i.e., outlier genes) can bias phylogenetic reconstruction (Kimball et al. 2013; Shen
517 et al. 2017). We noted several potential outliers within these datasets (Table S3). As indicated
518 above, some outliers can significantly support certain hypotheses. However, removal of most
519 single outlier genes did not change the results significantly nor could we detect any alignment
520 errors with these genes. The diversity of alternative hypotheses noted earlier made it difficult to
521 detect the underlying reasons for biased support from outliers. One biological process that might
522 cause biased phylogenetic resolution is selection. However, we could not test selection as most
523 exons contained premature stop codons (e.g., single mutation likely caused by sequencing or
524 assembly error). Both introns and UCEs also contain outliers. Although it was impossible to link
525 gene specific traits to the topology they support without annotation, our categorical EBA indeed
526 implied that the earliest diverging taxa in Neoaves might be influenced by outlier signal. In
527 contrast to the case for the earliest diverging Neoaves, we did not detect as strong of an impact
528 from outlier genes on the other two focal edges (the positions of Hoatzin and owls).
529
530 ***3.5 Within gene region conflict***
531 To determine whether gene tree conflict was the result of conflicting signal within genomic
532 regions, we further examined phylogenetic signal across regions within each gene. The average
533 gene-region length of the Jarvis data was 1998 bp (501 – 15819 bp) for exons, 2509 bp (1787 –
534 3527 bp) for UCEs, and s 9309 bp (506 – 66,762 bp) for introns. For Prum data, the average
535 gene region length was 1524 bp (361 – 2316 bp). We focused on exon and UCE alignments as
536 they were smaller and therefore less likely than introns to suffer from mixed signal. We
537 conducted analyses on each gene region to determine whether 1000 bp segments conflicted with

538 the ML tree calculated for the entire region. We found extensive conflicting signal after
539 collapsing edges with < 95% UFBS and < 80% SH-aLRT support. Although this is an extremely
540 conservative measure, and likely to have a high false-negative rate (Guindon et al. 2010), it was
541 chosen to prevent false positives. For loci with at least 2 × 1000 bp segments, we found that 10%
542 of Jarvis et al. (2014) exons (195 of 1985), 6% (207 of 3367) of UCEs, and 50% (8 of 15) of
543 gene regions in Prum et al. (2015) had conflicts. It is noteworthy that exons in Jarvis et al. (2014)
544 usually concatenated multiple exon regions of one gene and that some of those exons are
545 separated by long introns. Thus, those exons might exhibit different evolutionary histories due to
546 recombination, selection, and/or other reasons. Despite the complexity of the Jarvis exons, the
547 number of conflicts we observed in this analysis was only slightly higher than it was for UCEs.
548 Although intragenic conflicts within the Prum data were much higher, they could reflect
549 sampling error due to the small number (i.e., only 15) of long gene regions in the data; the larger
550 number of taxa in the Prum dataset is also likely to have had an impact.
551 To determine whether within gene conflict corresponded to obvious data "dirtiness", we
552 examined alignments for gene regions that exhibited conflict. All large datasets suffer from some
553 amount of noisy data (Springer and Gatesy 2018; Braun et al. 2019) and we did find some cases
554 where intragenic conflicts might reflect misalignment. For example, the 1424.exon gene region
555 from Jarvis et al. (2014) had an obviously "messy" alignment (Fig. S6); analyses of problematic
556 segments placed Rifleman sister to pelicans, mesites sister to cranes, grebes sister to sandgrouse,
557 and fulmars sister to seriemas. However, many other loci that exhibited substantial intragenic
558 conflicts had alignments that appear largely unambiguous (e.g., locus 9838.exons, Fig. S6),
559 which suggests potential biological processes, like those highlighted by Scornavacca and Galtier
560 (2017) and Mendes et al. (2019), underlie the observed intragenic conflicts.
561
562 ***3.6 Simulations***
563 Most of the gene-tree topologies resulted in a single species/lineage as sister to the remaining
564 lineages (Figs. 2B and S3). To determine if this may be expected given that short internodes
565 should have a higher prevalence of ILS, we conducted coalescent simulations using the MP-
566 EST* TENT tree from Jarvis et al. (2014). This tree has a clade **VI+VII** as the earliest diverged
567 Neoaves, the Hoatzin groups with a large clade including **II**+**III**+*S*+*CR*, and owls are sister to
568 *EHV*. We call to the relationships in this tree the *true model relationships*. We found the overall

level of ILS to be relatively high (~58 ARFD between the simulated gene trees and the model species tree). GTEE also appeared to be high, showing ~68 unweighted RF distances between the simulated gene trees and the ML estimates of simulated gene trees, which implies low phylogenetic signal per gene for reconstructing this rapid Neoavian radiation. Even though, coalescent species-trees reconstructed with ASTRAL III using simulated data did recover > 90% of the true model relationships across the tree, the concatenation analyses only recovered ~85% of the true model relationships (Table S4). However, the positions of the Hoatzin and the earliest diverging Neoavian lineage differed from the true model topologies 61% and 44% of the time, respectively, possibly due to the high GTEE and ILS.

The most common topologies for each focal edge in the ML estimates of simulated gene trees were likely to have a single species/lineage sister to the remaining clades (Fig. S7). We conducted EBA for 184 bipartition constraints (see Methods 2.5) using the simulated alignments. Among the bipartitions, there were 63 (earliest Neoaves), 45 (Hoatzin sister), and 14 (owl sister) conflicting hypotheses for each of focal edge (Table 3). The best supported hypotheses usually differed from the true model relationships (Table 3). For example, for the earliest diverging Neoaves, 25 and 28 hypotheses obtained some support from the two sets of simulated exons, respectively. Among them, the model topology (**VI+VII** as earliest Neoaves) is only supported by one or five genes and ranked as the 14th or 18th among the resolutions. The situation was similar for simulated introns and UCEs (Table 3) and for the other two focal edges: the model topology ranks 10th – 17th among the resolutions of the position of the Hoatzin and it ranks second for the position of owls (Table 3) across all data types.

In contrast to the focal edges, which were chosen because they exhibited extremely short internodes and dramatic gene tree conflicts, we found that less contentious edges that are united by relatively long internodes (i.e., those with a low level of ILS) received high support across the simulations regardless of data type (Table 3). Examples of these cases included clades **I**, **II**, **III**, and **V** (Fig. 3A), which have been recovered in many previous studies. These clades indicate that EBA can recover the correct relationships when there is sufficient phylogenetic signal and limited ILS. However, the ML estimates of the simulated gene trees can exhibit a surprisingly high degree of disagreement with some strongly corroborated clades. For example, ~20% of the ML estimates of the simulated gene trees failed to recover the (Palaeognathae + Galloanserae) | Neoaves bipartition (i.e., some lineages within Neoaves were sister to Galloanserae). This may

seem surprising since the coalescent branch length leading to Neoaves on the model species tree is relatively long (2.03 coalescent units), but we confirmed this level of conflict with the species tree is expected given the multispecies coalescent by examining the simulated gene trees. However, we also note that the amount of ILS in the simulations depends on the coalescent branch lengths estimated by Jarvis et al. (2014). Coalescent branch length calculation is challenging (Forthman et al. 2022) and it is possible that Jarvis et al. (2014) underestimated the coalescent branch lengths; In fact, there is evidence from indels (Houde et al. 2020) that the true coalescent branch length is longer (2.57 coalescent units). Thus, our results represent the behavior of EBA for the case where most incongruence among estimated gene trees reflects ILS rather than GTEE. Nevertheless, the simulations provide guidance regarding the types of errors we might expect for EBA.

3.7 Potential limitations of edge-based analyses (EBA)

EBA can be used to assess the relative support for distinct hypotheses, but it does have some limitations. Specifically, edge-based tests are difficult to perform if one wishes to examine a large number of edges (and/or hypotheses regarding the selected edges) due to the high computational load of this approach. This computational burden reflects the need to conduct preliminary tree searches to define the most plausible hypotheses as well as the constrained tree searches. We note that EBA can be viewed as extending another edge-based test, the SH-aLRT (approximate likelihood-ratio test with the nonparametric SH correction, Guindon et al. 2010). The SH-aLRT is used to assess support for edges by comparing the likelihood of the optimal tree with the two alternative trees produced by NNI (Table 1) moves. EBA extends this idea from NNIs to alternatives that: 1) have *a priori* support; or 2) are relatively common in the set of gene trees generated for phylogenomic datasets. Although this makes EBA more flexible it is difficult to devise approximations, like limiting re-optimization to the five edge lengths closest to the focal edge in the optimal tree (which is done in the SH-aLRT).

Another limitation of EBA is the fact the likelihood component of the analyses ($\Delta \ln L$) still relies on the substitution model selected for each gene. Obviously, model misspecification can still have an impact on tree topology. In this study, we used the most complex model – time-reversible model (GTR) – to overcome GTEE due to overly simplistic models, but it remains possible that the GTR model is itself inadequate, at least for some loci, so even more complex

631 models should be considered in the future. Another concern in revealed by our simulations is a
632 potential bias toward resolutions of edges that have a single species or lineage sister to the focal
633 taxon, although our simulations are likely to represent a case where ILS is overestimated and
634 GTEE is underestimated. The major benefit of EBA is that it provides information about the
635 support for alternatives to the best-corroborated resolution for each focal edge. Overall, these
636 considerations suggest that EBA might be most appropriate for questions where the number of
637 difficult nodes is limited, when the sets of plausible alternative hypotheses are small, and when
638 one wishes to understand the relative support for each of those plausible alternatives.
639
640 **4. Conclusions**
641 The categorical EBA conducted herein provide a way to examine differences in signal associated
642 with subsets of the data and assess the best-supported resolution of specific nodes. The best-
643 corroborated resolutions of our focal nodes were: 1) owl + *M*; 2) Hoatzin + *S*; and 3) doves are
644 the earliest diverging Neoaves. The best-corroborated hypothesis for owl and Hoatzin was much
645 better supported than the alternatives for all three data types (Fig. 4), although the EBA still
646 revealed substantial conflict. The conflicts evident in the EBA were more complex than the
647 conflicts among analyses of different data types in Jarvis et al. (2014), Reddy et al. (2017), and
648 Braun and Kimball (2021). First, the owls + *EHV* conflict reflects the interaction of GC_{CV} and
649 data type, rather than data type *per se*. Second, the position of Hoatzin was highly variable but
650 there was a data type effect that was not evident in previous studies. Specifically, support for
651 Hoatzin + **V** was strongest in introns, intermediate in UCEs, and weakest for exons. Finally, data
652 type effects were evident for the earliest diverging Neoaves, as expected based on Reddy et al.
653 (2017) and Braun and Kimball (2021), but outlier genes also appeared to play an important role
654 in this part of the tree. There was not a single factor (e.g., GC_{CV} or data type) that played an
655 important role in the resolution of all three focal nodes. Thus, simple solutions like focusing on a
656 specific data type or eliminating genes with high GC_{CV} are unlikely to be a panacea for analyses
657 of avian phylogeny (or, by extension, other nodes in the Tree of Life that have proven to be
658 recalcitrant). We believe that our findings will facilitate further exploration of phylogenetic
659 conflicts using an edge-by-edge approach.
660 Perhaps one of the most surprising results of this study is the fact that the results of the
661 EBA for the earliest divergence within Neoaves contradict monophyly for two of the magnificent

662 seven clades, which are the superordinal groups that have been consistently identified on the
663 Neoavian tree by recent large-scale studies (Reddy et al. 2017). The consistent recovery of the
664 magnificent seven has led to the view that most or all of these clades are present in the true avian
665 species tree (Suh 2016; Braun et al. 2019; Sangster et al. 2022). However, EBA indicate that at
666 least some of those groups might have less support than we currently believe. For example,
667 signal placing either cuckoos or doves sister to all other Neoaves is stronger than many other
668 alternatives (Figs. 4 and 5). However, the cuckoos sister signal contradicts magnificent seven
669 clade **IV** and the doves sister signal contradicts clade **VI**. There are several interpretations of this
670 result. First, clades **IV** and **VI** could both be present in the true tree, but the conflicting signals
671 evident in EBA reflect the fact that the branches uniting clades **V** and **VI** are especially short and,
672 therefore, "noisy" (e.g., due to ILS). Arguably, this is the simplest hypothesis given that
673 essentially all previous studies (e.g., Jarvis et al. 2014; Prum et al. 2015; Braun and Kimball
674 2021; Kuhl et al. 2021) agree that the relevant edges are quite short. Second, the fact that signals
675 contradicting those magnificent seven clades are stronger than signals consistent with those
676 clades could provide evidence that clades **IV** and **VI** are present but there is something unusual
677 about the branches uniting those clades. In fact, Houde et al. (2020) examined indel data and
678 they reported that the proportion of indels that conflict with the branch uniting clade **VI** was
679 higher than expected given the relevant edge length in the Jarvis et al. (2014) time tree; they
680 interpreted this as evidence for a transient increase in the effective population size for the
681 common ancestor of that clade. Finally, EBA can be viewed as evidence that the true bird tree
682 lacks either clade **IV** (if the signal supporting the "cuckoos sister" hypothesis is correct) or clade
683 **VI** (if the signal supporting the "doves sister" hypothesis is correct). Indeed, Braun and Kimball
684 (2021) explicitly questioned clade **IV** and Sangster et al. (2022) excluded clade **IV** from the set
685 of strongly corroborated clades (instead, Sangster et al. [2022] named a subset of clade **IV**).
686 These EBA further emphasize the uncertainty regarding clades **IV** and **VI**. Regardless of the best
687 interpretation of the EBA, they provide a way to highlight especially problematic branches that
688 warrant further examination in future phylogenomic studies.
689 Given the evidence for conflict evident in our EBA we are left with a fundamental
690 question: what is the best-way forward for resolving the nodes in the bird tree that remain
691 uncertain? Obviously, collecting even more data will be important and efforts like the B10K
692 (Zhang 2015; Stiller and Zhang 2019) and the OpenWings (Kimball et al. 2019) projects will

provide these larger datasets for birds. However, there is ample evidence that simply expanding the size of phylogenomic datasets will not solve the problem of recalcitrant nodes in avian phylogeny (or the difficult nodes in other parts of the tree of life). Rare genomic changes (Rokas and Holland 2000) may provide an alternative data type that sidesteps the complexities evident in the analyses we present here. In fact, rare genomic changes can avoid (or at least reduce) problems like intralocus recombination, natural selection, and GTEE (Springer and Gatesy 2019). The availability of genome-scale datasets will only increase availability of rare genomic change data and allow the community to move beyond retroposon insertions, which were used even before the phylogenomic era (e.g., Suh et al. 2011), to types of rare genomic changes like numts (Liang et al. 2018) and microinversions (Braun et al. 2011) that have not been used in many phylogenetic studies. These types of data, which are very different from nucleotide sequence data, have the potential to corroborate (or falsify) the hypothesis that the most common resolution in EBA represents a correct resolution of the species tree (at least for some data types). Regardless of whether the hypothesis with the greatest support (whether judged using $\sum\Delta\ln L$ and $\sum$Ng) is correct, EBA reveal substantial conflicts within the data. Understanding those conflicts is an important problem in evolutionary biology even if we do not know the true resolution of the tree. We can learn even more if the information about conflicts among genes, like those revealed by our EBA, can be combined with an accurate estimate of the species tree.

Supplementary material

Supplementary figures and tables can be found online.

Acknowledgements

We would like to thank Benjamin Winger, Joseph Walker, Nathanael Walker-Hale and Diego Alvarado-Serrano for their constructive comments on the earliest version of the paper. We appreciate other comments from members of the Smith lab and valuable comments from the two anonymous reviewers. This work is supported by grants from the US National Science Foundation (DBI-1458466 and DEB-1207915 to S.A.S., DEB-1241066 and DEB-1146423 to J.C., and DEB-1655683 to E.L.B.), the National Natural Science Foundation of China (No. 32160114 to B.L. and No. 32170460 to N.W.), and by the Frank M. Chapman Memorial Fund of the American Museum of Natural History. N.W. is also supported by Young science and

technology talents cultivation project of Inner Mongolia University (No. 21221505).

Author contributions

Study conception and design: N.W., S.A.S.; Acquisition of data: N.W.; Analysis and interpretation of data: N.W., S.A.S., E.L.B., J.C., B.L.; Drafting of manuscript: N.W., E.L.B., J.C., S.A.S.; Image illustration: B.L., N.W., E.L.B., J.C.

Competing interests

The authors have no competing interests declared.

References

Braun EL, Kimball RT, Han KL, Iuhasz-Velez NR, Bonilla AJ, Chojnowski JL, Smith JV, Bowie RC, Braun MJ, Hackett SJ, Harshman J. 2011. Homoplastic microinversions and the avian tree of life. *BMC Evol Biol.* 11(1):141.

Braun EL, Cracraft J, Houde P. 2019. Resolving the avian tree of life from top to bottom: the promise and potential boundaries of the phylogenomic era. In Avian Genomics in Ecology and Evolution (pp. 151-210). Springer, Cham.

Braun EL, Kimball RT. 2021. Data types and the phylogeny of Neoaves. *Birds* 2(1):1-22.

Bryant D, Hahn MW. 2020. The concatenation question. in: Scornavacca C., Delsuc, F., Galtier N. (Eds.). Phylogenetics in the Genomic Era, No commercial publisher | Authors open access book, pp.3.4:1–3.4:23. hal-02535651f.

Chen D, Braun EL, Forthman M, Kimball RT, Zhang Z. 2018. A simple strategy for recovering ultraconserved elements, exons, and introns from low coverage shotgun sequencing of museum specimens: Placement of the partridge genus *Tropicoperdix* within the galliformes. *Mol Phylogenet Evol.* 129:304–314.

Chojnowski JL, Kimball RT, Braun EL, 2008. Introns outperform exons in analyses of basal avian phylogeny using clathrin heavy chain genes. *Gene* 410(1):89–96.

Domínguez-Bello MG, Michelangeli F, Ruiz MC, Garcia A, Rodriguez E. 1994. Ecology of the folivorous hoatzin (*Opisthocomus Hoatzin*) on the Venezuelan plains. *Auk* 111(3):643–651.

Duchêne DA, Duchêne S, Ho SYW. 2017. New statistical criteria detect phylogenetic bias caused by compositional heterogeneity, *Mo Biol Evol*, 4(6): 1529–1534

Duchêne DA, Tong KJ, Foster CS, Duchene S, Lanfear R, Ho SYW. 2018. Linking branch lengths across loci provides the best fit for phylogenetic inference. *bioRxiv* 467449.

Edwards SV. 2009. Is a new and general theory of molecular systematics emerging? *Evolution* 63(1):1-19.

Edwards SV, Xi Z, Janke A, Faircloth BC, McCormack JE, Glenn TC, Zhong B, Wu S, Lemmon EM, Lemmon AR, Leaché AD. 2016. Implementing and testing the multispecies coalescent model: a valuable paradigm for phylogenomics. *Mol Phylogenet Evol.* 94: 447-462.

Ericson PG, Anderson CL, Britton T, Elzanowski A, Johansson US, Källersjö M, Ohlson JI, Parsons TJ, Zuccon D, Mayr G. 2006. Diversification of Neoaves: integration of molecular sequence data and fossils. *Biol Lett.* 2(4):543–547.

Foster PG, Hickey DA. 1999. Compositional bias may affect both DNA-based and protein-based phylogenetic reconstructions. *J Mol Evol.* 48:284–290.

Galtier N, Gouy M. 1998. Inferring pattern and process: maximum-likelihood implementation of a nonhomogeneous model of DNA sequence evolution for phylogenetic analysis. *Mol Biol Evol.* 15(7): 871-879.

Gatesy J, Springer MS. 2017. Phylogenomic red flags: Homology errors and zombie lineages in the evolutionary diversification of placental mammals. *Proc Natl Acad Sci USA.* 114(45):E9431–E9432.

Gilbert PS, Wu J, Simon MW, Sinsheimer JS, Alfaro ME. 2018. Filtering nucleotide sites by phylogenetic signal to noise ratio increases confidence in the Neoaves phylogeny generated from ultraconserved elements. *Mol Phylogenet Evol.* 126:116–128.

Gordon EL, Kimball RT, Braun EL. 2021. Protein structure, models of sequence evolution, and data type effects in phylogenetic analyses of mitochondrial data: A case study in birds. *Diversity* 13:555.

Guindon S, Dufayard JF, Lefort V, Anisimova M, Hordijk W, Gascuel O. 2010. New algorithms and methods to estimate maximum-likelihood phylogenies: assessing the performance of PhyML 3.0. *Syst Biol.* 59(3):307–321.

Hackett SJ, Kimball RT, Reddy S, Bowie RC, Braun EL, Braun MJ, Chojnowski JL, Cox WA, Han KL, Harshman J, Huddleston CJ. et al. 2008. A phylogenomic study of birds reveals their evolutionary history. *Science* 320(5884):1763–1768.

Hillis DM, Bull JJ. 1993. An empirical test of bootstrapping as a method for assessing confidence in phylogenetic analysis. *Syst Biol.* 42(2):182–192.

Hoang DT, Chernomor O, Von Haeseler A, Minh BQ, Vinh LS. 2018 UFBoot2: Improving the ultrafast bootstrap approximation. *Mol Biol Evol.* 35:518–522.

Holland BR, Jarvis PD, Sumner JG. 2013. Low-parameter phylogenetic inference under the general Markov model. *Syst Biol.* 62:78-92.

790 Hughes JM, Baker AJ. 1999. Phylogenetic relationships of the enigmatic hoatzin (*Opisthocomus Hoatzin*)
791 resolved using mitochondrial and nuclear gene sequences. *Mol Biol Evol.* 16(9):1300–1307.
792 Houde P, Braun EL, Narula N, Minjares U, Mirarab S. 2019. Phylogenetic signal of indels and the
793 neoavian radiation. *Diversity* 11(7):108.
794 Houde P, Braun EL, Zhou L. 2020. Deep-time demographic inference suggests ecological release as
795 driver of Neoavian adaptive radiation. *Diversity* 12:164.
796 Jarvis ED, Mirarab S, Aberer AJ, Li B, Houde P, Li C, Ho SY, Faircloth BC, Nabholz B, Howard JT, Suh
797 A. et al. 2014. Whole-genome analyses resolve early branches in the tree of life of modern birds.
798 *Science* 346(6215):1320–1331.
799 Jarvis ED, Mirarab S, Aberer AJ, Li B, Houde P, Li C, Ho SY, Faircloth BC, Nabholz B, Howard JT, Suh
800 A. et al. 2015. Phylogenomic analyses data of the avian phylogenomics project. *GigaScience*
801 4(1):4.
802 Jermiin LS, Ho SY, Ababneh F, Robinson J, Larkum AW. 2004. The biasing effect of compositional
803 heterogeneity on phylogenetic estimates may be underestimated. *Syst Boil*. 53(4):638-643.
804 Kimball RT, Wang N, Heimer-McGinn V, Ferguson C, Braun EL. 2013. Identifying localized biases in
805 large datasets: a case study using the avian tree of life. *Mol Phylogenet Evol.* 69(3): 1021–1032.
806 Kimball RT, Oliveros CH, Wang N, White ND, Barker FK, Field DJ, Ksepka DT, Chesser RT, Moyle
807 RG, Braun MJ, Brumfield RT, Faircloth BC, Smith BT, Braun EL. 2019. A phylogenomic
808 supertree of birds. *Diversity* 11(7):109
809 Kobert K, Salichos L, Rokas A, Stamatakis A. 2016. Computing the internode certainty and related
810 measures from partial gene trees. *Mol Biol Evol.* 33(6):1606-1617.
811 Kolaczkowski B, Thornton JW. 2004. Performance of maximum parsimony and likelihood phylogenetics
812 when evolution is heterogeneous. *Nature* 431(7011):980.
813 Kubatko LS, Degnan JH. 2007. Inconsistency of phylogenetic estimates from concatenated data under
814 coalescence. *Syst Biol.* 56(1):17–24.
815 Kuhl H. Frankl-Vilches C, Bakker A, Mayr G, Nikolaus G, Boerno ST, Klages S, Timmermann B, Gahr,
816 M. 2021. An unbiased molecular approach using 3′-UTRs resolves the avian family-level tree of
817 life. *Mol Biol Evol.* 38(1):108-127.
818 Li Y, Liu Z, Shi P, Zhang J. 2010. The hearing gene Prestin unites echolocating bats and whales. *Curr*
819 *Biol.* 20(2):R55-R56
820 Liang B, Wang N, Li N, Kimball RT, Braun EL. 2018. Comparative genomics reveals a burst of
821 homoplasy-free numt insertions. *Mol Biol Evol.* 35(8):2060–2064.
822 Liu L, Yu L, Edwards SV. 2010. A maximum pseudo-likelihood approach for estimating species trees
823 under the coalescent model. *BMC Evol Biol.* 10(1):302.

824 Liu L, Zhang J, Rheindt FE, Lei F, Qu Y, Wang Y, Zhang Y, Sullivan C, Nie W, Wang J, Yang F. 2017.
825 Reply to Gatesy and Springer: Claims of homology errors and zombie lineages do not
826 compromise the dating of placental diversification. *Proc Natl Acad Sci USA*. 114(45):E9433–
827 E9434.
828 McCormack JE, Harvey MG, Faircloth BC, Crawford NG, Glenn TC, Brumfield RT. 2013. A phylogeny
829 of birds based on over 1,500 loci collected by target enrichment and high-throughput
830 sequencing. *PLoS One* 8(1):e54848.
831 Mendes FK, Livera AP, Hahn MW. 2019. The perils of intralocus recombination for inferences of
832 molecular convergence. *Philos Trans Royal Soc B*. 374(1777):20180244.
833 Minh BQ, Nguyen MA, von Haeseler A. 2013. Ultrafast approximation for phylogenetic bootstrap. *Mol*
834 *Biol Evol.* 30(5):1188–1195.
835 Mirarab S, Bayzid MS, Boussau B, Warnow T. 2014. Statistical binning enables an accurate coalescent-
836 based estimation of the avian tree. *Science* 346(6215).
837 Molloy EK, Warnow T. 2018. To include or not to include: the impact of gene filtering on species tree
838 estimation methods. *Syst Biol.* 67(2):285-303.
839 Morgan CC, Foster PG, Webb AE, Pisani D, McInerney JO, O'Connell MJ. 2013. Heterogeneous models
840 place the root of the placental mammal phylogeny. *Mol Biol Evol.* 30(9):2145–2156.
841 Mount GG, Brown JM. 2022. Comparing likelihood ratios to understand genome-wide variation in
842 phylogenetic support. *Syst Biol.* syac014. doi: 10.1093/sysbio/syac014.
843 Nguyen LT, Schmidt HA, von Haeseler A, Minh BQ. 2014. IQ-TREE: a fast and effective stochastic
844 algorithm for estimating maximum-likelihood phylogenies. *Mol Biol Evol.* 32(1):268–274.
845 Pandey A, Braun EL. 2020. Phylogenetic analyses of sites in different protein structural environments
846 result in distinct placements of the Metazoan root. *Biology* 2020, *9*:64.
847 Prum RO, Berv JS, Dornburg A, Field DJ, Townsend JP, Lemmon EM, Lemmon AR. 2015. A
848 comprehensive phylogeny of birds (Aves) using targeted next-generation DNA
849 sequencing. *Nature* 526(7574):569.
850 Puttick MN, Morris JL, Williams TA, Cox CJ, Edwards D, Kenrick P, Pressel S, Wellman CH, Schneider
851 H, Pisani D, Donoghue PC. 2018. The interrelationships of land plants and the nature of the
852 ancestral embryophyte. *Curr Biol.* 28(5):733–745.
853 Rambaut A, Grass NC. 1997. Seq-Gen: an application for the Monte Carlo simulation of DNA sequence
854 evolution along phylogenetic trees. *Bioinformatics* 13(3):235–238.
855 Reddy S, Kimball RT, Pandey A, Hosner PA, Braun MJ, Hackett SJ, Han KL, Harshman J, Huddleston
856 CJ, Kingston S, Marks BD. 2017. Why do phylogenomic data sets yield conflicting trees? Data
857 type influences the avian tree of life more than taxon sampling. *Syst Biol.* 66(5):857–879.

Robinson DF, Foulds LR. 1981. Comparison of phylogenetic trees. *Math Biosci.* 53(1-2):131–147.

Rokas A, Holland PW. 2000. Rare genomic changes as a tool for phylogenetics. *Trends Ecol Evol.* 15(11):454–459.

Salichos L, Stamatakis A, Rokas A. 2014. Novel information theory-based measures for quantifying incongruence among phylogenetic trees. *Mol Biol Evol.* 31:1261–1271.

Sangster G, Braun EL, Johansson US, Kimball RT, Mayr G, Suh A. 2022. Phylogenetic definitions for 25 higher-level clade names of birds. *Avian Res.* 100027.

Scornavacca C, Galtier N. 2017. Incomplete lineage sorting in mammalian phylogenomics. *Syst Biol.* 66(1):112–120.

Shen XX, Hittinger CT, Rokas A. 2017. Contentious relationships in phylogenomic studies can be driven by a handful of genes. *Nat Ecol Evol.* 1(5): 0126.

Simmons M.P., Sloan D.B., Gatesy J. 2016. The effects of subsampling gene trees on coalescent methods applied to ancient divergences. *Mol Phylogenet Evol.* 97:76–89.

Smith SA, Walker-Hale N, Walker JF, Brown J. 2020. Phylogenetic Conflicts, Combinability, and Deep Phylogenomics in Plants. *Syst Biol.* 69(3):579–592.

Springer MS, Gatesy J. 2016. The gene tree delusion. *Mol Phylogenet Evol.* 94:1–33.

Springer MS, Gatesy J. 2018. On the importance of homology in the age of phylogenomics. *System Biodivers.* 16(3): 210-228.

Springer MS, Gatesy J 2019. Retroposon insertions within a multispecies coalescent framework suggest that ratite phylogeny is not in the 'Anomaly Zone'. *bioRxiv* p.643296.

Stamatakis A. 2014. RAxML Version 8: A tool for Phylogenetic Analysis and Post-Analysis of Large Phylogenies. *Bioinformatics* 30 (9):1312-1313.

Stiller J, Zhang G. 2019. Comparative phylogenomics, a stepping stone for bird biodiversity studies. *Diversity* 11: 115.

Suh A. 2016. The phylogenomic forest of bird trees contains a hard polytomy at the root of Neoaves. *Zool Scr.* 45:50–62.

Suh A, Paus M, Kiefmann M, Churakov G, Franke FA, Brosius J, Kriegs JO, Schmitz J. 2011. Mesozoic retroposons reveal parrots as the closest living relatives of passerine birds. *Nat Commun.* 2:443.

Suh A, Linnéa S, Hans E. 2015. The dynamics of incomplete lineage sorting across the ancient adaptive radiation of neoavian birds. *PLoS Biol.* 13(8):e1002224.

Sukumaran J, Holder MT. 2010. DendroPy: A Python library for phylogenetic computing. *Bioinformatics* 26:1569–1571.

890 Tarver JE, Dos Reis M, Mirarab S, Moran RJ, Parker S, O'Reilly JE, King BL, O'Connell MJ, Asher RJ,
891 Warnow T, Peterson KJ. 2016. The interrelationships of placental mammals and the limits of
892 phylogenetic inference. *Genome Biol Evol.* 8(2):330–344.
893 Wang K, Wang J, Zhu C, Yang L, Ren Y, Ruan J, Fan G, Hu J, Xu W, Bi X, Zhu Y. 2021. African
894 lungfish genome sheds light on the vertebrate water-to-land transition. Cell. 184(5):1362-76.
895 Wang N, Braun EL, Kimball RT. 2012. Testing hypotheses about the sister group of the Passeriformes
896 using an independent 30-locus data set. *Mol Biol Evol.* 29(2):737–750.
897 Wang N, Kimball RT, Braun EL, Liang B, Zhang Z. 2017. Ancestral range reconstruction of Galliformes:
898 the effects of topology and taxon sampling. *J Biogeogr.* 44(1):122–135.
899 Wang N, Yang Y, Moore MJ, Brockington SF, Walker JF, Brown JW, Liang B, Feng T, Edwards C,
900 Mikenas J, Olivieri J. et al. 2019. Evolution of Portulacineae marked by gene tree conflict and
901 gene family expansion associated with adaptation to harsh environments. *Mol Biol Evol.*
902 36(1):112–126.
903 Wickett NJ, Mirarab S, Nguyen N, Warnow T, Carpenter E, Matasci N, Ayyampalayam S, Barker MS,
904 Burleigh JG, Gitzendanner MA, Ruhfel BR. et al. 2014. Phylotranscriptomic analysis of the
905 origin and early diversification of land plants. *Proc Natl Acad Sci USA.* 111(45):E4859–E4868.
906 Zhang GJ. 2015. Bird sequencing project takes off. *Nature* 522:34-44.
907 Zhang C, Rabiee M, Sayyari E, Mirarab S. 2018. ASTRAL-III: Polynomial time species tree
908 reconstruction from partially resolved gene trees. *BMC Bioinformatics* 19(6):153.
909

Table 1. Glossary of terms and abbreviations used in this study.

Term	Full name and explanation
EBA	edge-based analyses: constraint phylogenetic analyses on certain edge on the tree.
categorical EBA	categorical edge-based analyses
UCEs	Ultra-conserved elements
GCcv	GC content variation
ILS	Incomplete Lineage Sorting
BS	Bootstrap Support
UFBS	Ultra Fast Bootstrap Support
SH-aLRT	approximate likelihood-ratio test with the nonparametric SH correction
NNI	Nearest-neighbor interchange, which exchanges the connectivity of four subtrees within the main tree.
RF	Robinson-Foulds distances
TENT ExaML	the concatenated total evidence nucleotide tree from Jarvis et al. (2014)
ICA value	Internode Certainty All; the degree of certainty for a bipartition in a given set of trees in conjunction with all conflicting bipartitions in the same tree set
GTEE	gene-tree estimation error
$\ln L$	log likelihood score
$\Delta\ln L$	difference in $\ln L$ between the best and the second-best resolutions for each gene
$\sum\Delta\ln L$	summation of $\Delta\ln L$ for each constraint from supporting genes
sig$\Delta\ln L$	genes showing significant support for a specific topology (i.e., $\Delta\ln L > 2$)
$\sum$sig$\Delta\ln L$	summation of $\Delta\ln L$ among genes with significant support (i.e., $\Delta\ln L > 2$)
$\sum$Ng	the number of genes supporting a specific topology
EL/EH	exons with lower or higher ΔGC_{90}/tree length
IL/IH	introns with lower or higher ΔGC_{90}/tree length
UL/UH	UCEs with lower or higher ΔGC_{90}/tree length
ΔGC_{50}	the GC differences between taxa with high (the upper quartile) and low (the lower quartile) GC content.
ΔGC_{90}	the GC differences between taxa with high (the 95 percentile) and low (the 5 percentile) GC content.
ΔGC_{100}	the GC differences between taxa with the highest and the lowest GC content.

Avian lineages:	Also see Jarvis et al. (2014) and Sangster et al. (2022) for clade names
S	Shorebirds (Charadriiformes)
CR	Cranes and Rails (Gruiformes)
TB	Turacos and Bustards (Musophagotides)
M	Mousebirds (Coliiformes)
W	Woodpeckers and allies (Cavitaves)
EHV	Eagles, Hawks, and New World Vultures (Accipitriformes)
"Magnificent Seven"	Superordinal groups in Neoaves tree that have been recovered in almost all recent large-scale studies; we use Roman numerals to indicate these groups
I	Telluraves (Core Landbirds)
II	Aequornithes (Core Waterbirds)
III	Phaethontimorphae (Sunbittern, Kagu, and Tropicbirds)
IV	Otidimorphae (Cuckoos, Bustards, and Turacos)
V	Strisores/Caprimulgimorphae (Nightjars, Swifts, Hummingbirds, and allies)
VI	Columbimorphae (Doves, Mesites, and Sandgrouse)
VII	Phoenicopterimorphae/Mirandornithes (Flamingos and Grebes)

Table 2. Three focal edges and major testing hypotheses that published before.

Focal Edges	Hypotheses	Major References
Earliest Neoaves	1. **VI+VII**	Jarvis et al. 2014; Reddy et al. 2017; Braun and Kimball 2021
	2. **V**	Jarvis et al. 2014, Prum et al. 2015
	3. **VII**	Jarvis et al. 2014; Braun and Kimball 2021; Kuhl et al. 2021
	4. **III+V+VI+VII**	Hackett et al. 2008
	5. Doves	McCormack et al. 2013
Hoatzin's sister	1. **I+III+V**	Reddy et al. 2017
	2. **I**	Prum et al. 2015
	3. *S+CR*	Jarvis et al. 2014
	4. **V**	Jarvis et al. 2014
	5. *S*	McCormack et al, 2013, Jarvis et al. 2014
	6. *TB*	Jarvis et al. 2014
	7. **II+III**+*S+CR*	Jarvis et al. 2014
Owls' sister	1. *M+W*	Jarvis et al. 2014; Prum et al. 2015; Reddy et al. 2017
	2. *W*	McCormack et al. 2013; Jarvis et al. 2014
	3. *EHV*	Jarvis et al. 2014
	4. *M*	Hackett et al. 2008; Gilbert et al. 2018

NOTE.— the Greek numbers (bolded) correspond to the "magnificent seven" of Reddy et al. (2017), with other italic acronyms that can be referred to Table 1.

Table 3. Simulation results showing the best supported edge

Simulations	earliest Neoaves[1] (63[#])	TR	Hoatzin Sister[2] (45)	TR	Owls Sister[3] (14)	TR	**I** (33)	**II** (4)	**III** (16)	**V** (27)
exon1	Doves + Turacos	14	Sunbittern + Turacos	12	Owls + Mousebirds	2	**5432***	**19746**	**8497**	**5581**
exon2	Cuckoos + Sandgrouse	18	Sunbittern + Turacos	17	Owls + Mousebirds	2	**6438**	**15763**	**7757**	**5416**
intron1	Cuckoos + Doves	8	Sunbittern + Turacos	10	Owls + Mousebirds	2	**4639**	**21835**	**7672**	**6130**
intron2	Cuckoos + Sandgrouse	14	Sunbittern + Turacos	13	Owls + Mousebirds	2	**3805**	**14934**	**7122**	**6537**
UCE1	Cuckoos + Sandgrouse	14	Cranes + Flamingos + Grebes	13	Owls + Mousebirds	2	**4329**	**18031**	**7621**	**5733**
UCE2	Doves + Turacos	9	Hoatzin + Nightjars	17	Owls + Mousebirds	2	**5906**	**20108**	**7616**	**6508**

NOTE.— TR: the ranking of the model topology of each focal edge in the edge-based analyses. [#]: The number in the parenthesis represents the total number of conflicting constraints for each testing edge. [1]: showing the best hypothesis that is conflict with (**VI + VII**) + other Neoaves. [2]: showing the best hypothesis that is conflict with Hoatzin + **II** + **III** + *S* + *CR*. [3]: showing the best hypothesis that is conflict with Owls + *EHV*. Control edges include **I**, **II**, **III**, and **V**, which were all best supported by the edge-based analyses. *Bolded numbers: The difference of $\sum\Delta\ln L$ between the best hypotheses (i.e., **I, II, III, and V** respectively) and conflicting second best hypotheses for each edge. These large numbers indicate that the control edges can all be recovered with strong support. Clade keys can be found in Table 1 and Figure 3.

Figure Legends

Figure 1. Flow chart illustrating the analytical processes in the current study. Briefly, we used four types of sequence data (blue box, top) obtained from Jarvis et al (2014) and Prum et al. (2015) to examine the support for three selected edges in the avian tree of life (green box, left). Then we conducted two types of analyses using the sequence data (red box, center). First, we examined the resolutions of the three focal edges in gene trees. The results of those analyses (black box, right) were most common resolutions of the edges (upper pie chart) and information about the distribution of distances among gene trees (e.g., histogram of RF distances). Those results, combined with prior information from the literature, allowed us to define the set of plausible resolutions for each focal edge. EBA yields information about the relative support for each of those plausible resolutions; we present the relative support for each resolution either as a pie chart or as stacked column graphs (showing in the lower part of black box). The largest slice in this example pie chart (green) is the best-corroborated relationship, but the chart also shows three alternatives with substantial differences in their relative support. The interpretation of stacked column graphs is similar, but the use of columns makes it easier to compare differences in the relative support for various subsets of the data (in this example, data subsets A and B were compared).

Figure 2. A: Node support distribution among ML gene trees. B: Topology distribution of the ML gene trees for the three focal edges using Jarvis et al. (2014) exon data. Analyses for Introns and UCEs can be found in Figure S3. unsupported: relationships shown have less than 50% UFBS (ultrafast bootstrap support, we use lower support cutoff to show potential topology distributions). The Top 20 supported topologies are shown. rare resolutions: relationships shown in less than 10 gene trees. Hoatzin missing or Owl missing: Hoatzin or Owl is missing in the gene trees.

Figure 3. A: Keys (**I-VII**) for each major clade in the hypotheses being tested. B: flow chart on how to conduct edge-based analyses by using the earliest diverging Neoaves as an example.

Figure 4. The three focal edges and the testing hypotheses in the edges-based analyses using exons (upper), introns (middle) and UCEs (lower). A: The earliest diverging clade in Neoaves, including the five dominant hypotheses published before (1–5), and the five additional hypotheses prevalent observed in the gene trees for bias assessment (6–10). B: the sister of Hoatzin, including seven previously identified hypotheses. C: the sister group of Owls, including four commonly found hypotheses. $\sum\Delta\ln L$: the sum of log likelihood score differences; $\sum$Ng: the number of genes supporting a specific hypothesis. Hypotheses keys can be found in Figure 3.

Figure 5. A: The GC content variation among exons, introns, or UCEs, including ΔGC_{50}, ΔGC_{90}, and ΔGC_{100} (see Table 1 for explanation). B: Comparison of hypotheses supporting pattern between gene sets from the lower and upper quartile of ΔGC_{90} among data types. C: Tree length (left) and internode length (right) variation among different types of data. D: Comparison of hypotheses supporting pattern between gene sets from the lower and upper quartile of tree length variation. For x axis, EL/EH: exons with lower or higher ΔGC_{90}/tree length; IL/IH: introns with lower or higher ΔGC_{90}/tree length; UL/UH: UCEs with lower or higher ΔGC_{90}/tree length.

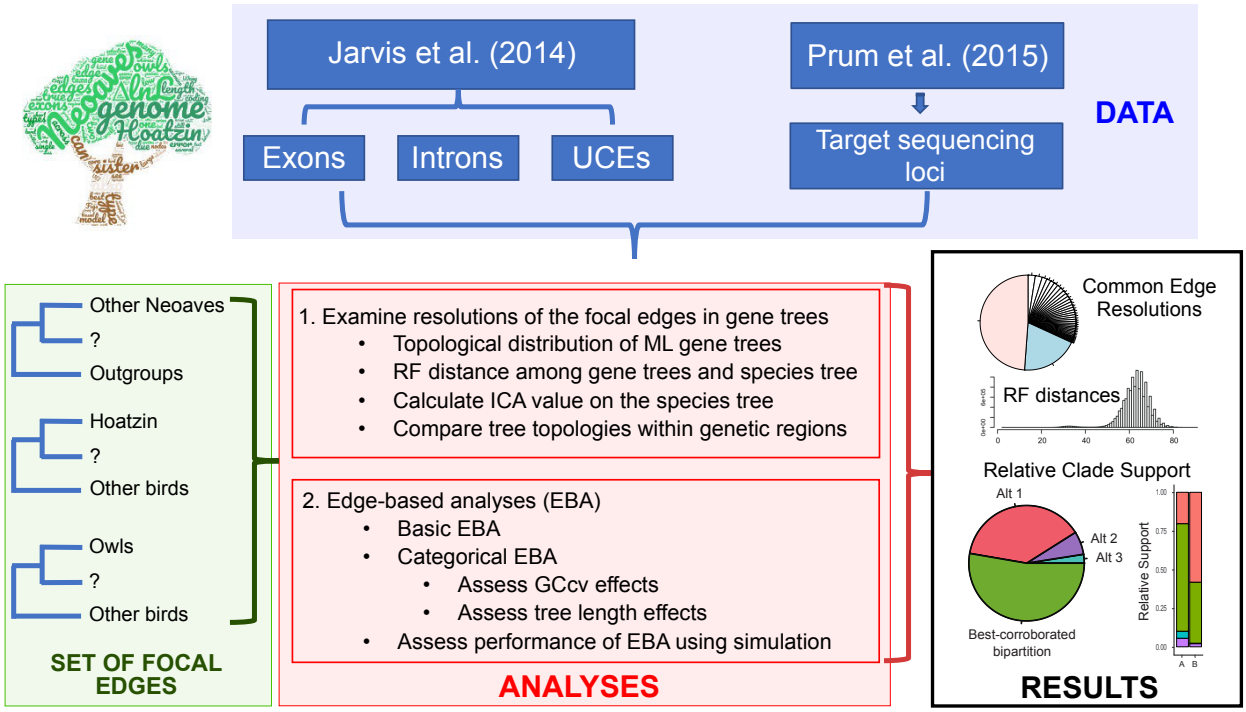
Jarvis et al. (2014)
Prum et al. (2015)
Exons
Introns
UCEs
Target sequencing loci
DATA
Other Neoaves
?
Outgroups
Hoatzin
?
Other birds
Owls
?
Other birds
SET OF FOCAL EDGES
1. Examine resolutions of the focal edges in gene trees
• Topological distribution of ML gene trees
• RF distance among gene trees and species tree
• Calculate ICA value on the species tree
• Compare tree topologies within genetic regions
2. Edge-based analyses (EBA)
• Basic EBA
• Categorical EBA
• Assess GCcv effects
• Assess tree length effects
• Assess performance of EBA using simulation
ANALYSES
Common Edge Resolutions
RF distances
Relative Clade Support
Alt 1
Alt 2
Alt 3
Best-corroborated bipartition
Relative Support
RESULTS

Figure 1

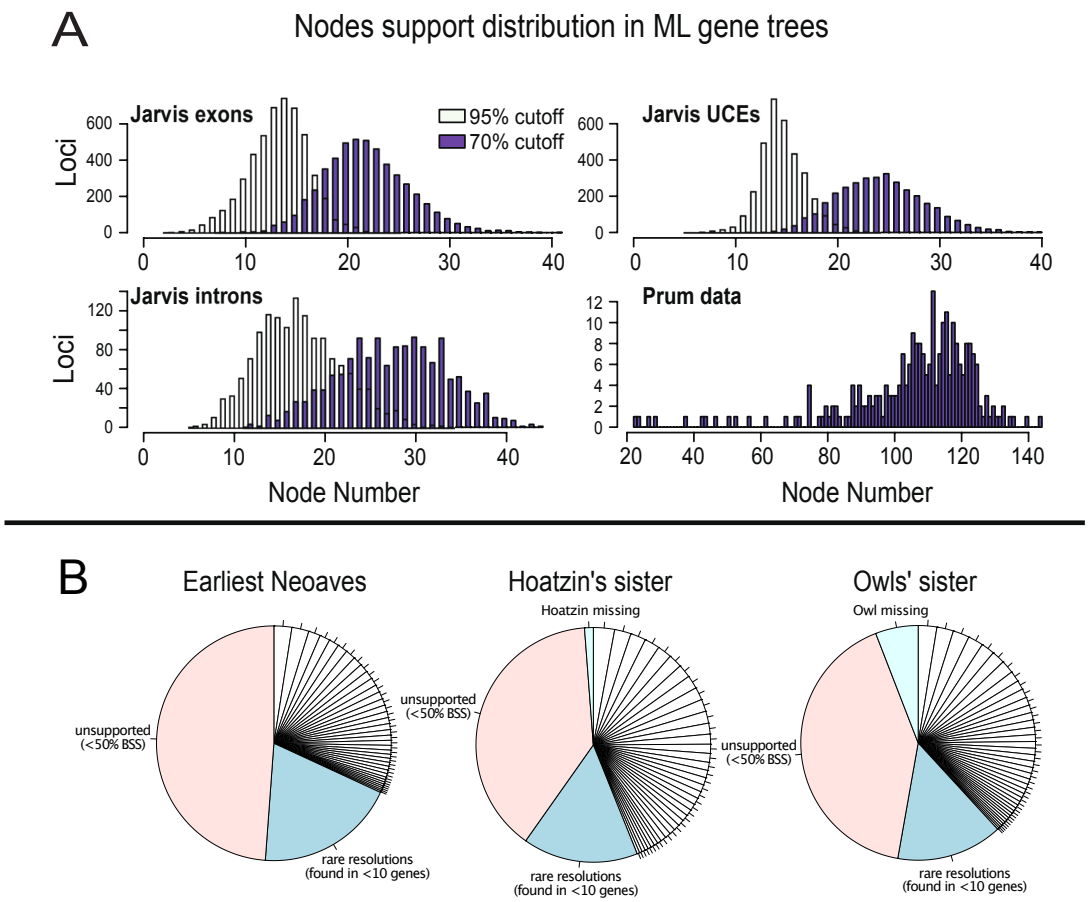

Top 20 topologies for each focal edge

Earliest diverging Neoaves	No. exons	Hoatzin's_sister	No. exons	Owls'_sister	No. exons
Hummingbirds & Swifts	125	Sunbittern	148	Eagles	130
Cuckoos	119	Plovers	115	Falcons	116
Doves	83	Cranes	107	Cuckoo-roller	114
Bustards	72	Turacos	106	Seriemas	106
Sandgrouse	70	Sandgrouse	100	Trogons	94
Mesites	70	Doves	95	New World Vultures	92
Parrots	70	Nightjars	93	Mousebirds	91
Woodpeckers	65	Bustards	93	Parrots	75
Tropicbirds	61	Cuckoos	89	Hornbills	64
Nightjars	58	Tropicbirds	85	Tropicbirds	63
Hoatzin	55	Mesites	84	Nightjars	56
Mousebirds	52	Falcons	76	Cranes	53
Cranes	52	Trogons	70	Bee-eaters	52
Passerines	46	Loons	64	Sunbittern	51
Plovers	46	Herons	62	Plovers	51
Turacos	43	Cuckoo-roller	56	Bustards	48
Falcons	42	Cormorants	52	Sandgrouse	47
Sunbittern	42	Seriemas	52	Mesites	45
Loons	38	Flamingos & Grebes	50	Hoatzin	45
Bee-eaters	36	Flamingos	50	Loons	44
Rare resolutions	976	Rare resolutions	803	Rare resolutions	740
Unsupported	2472	Unsupported	1975	Unsupported	2092
		Hoatzin missing	61	Owl missing	298

Figure 2

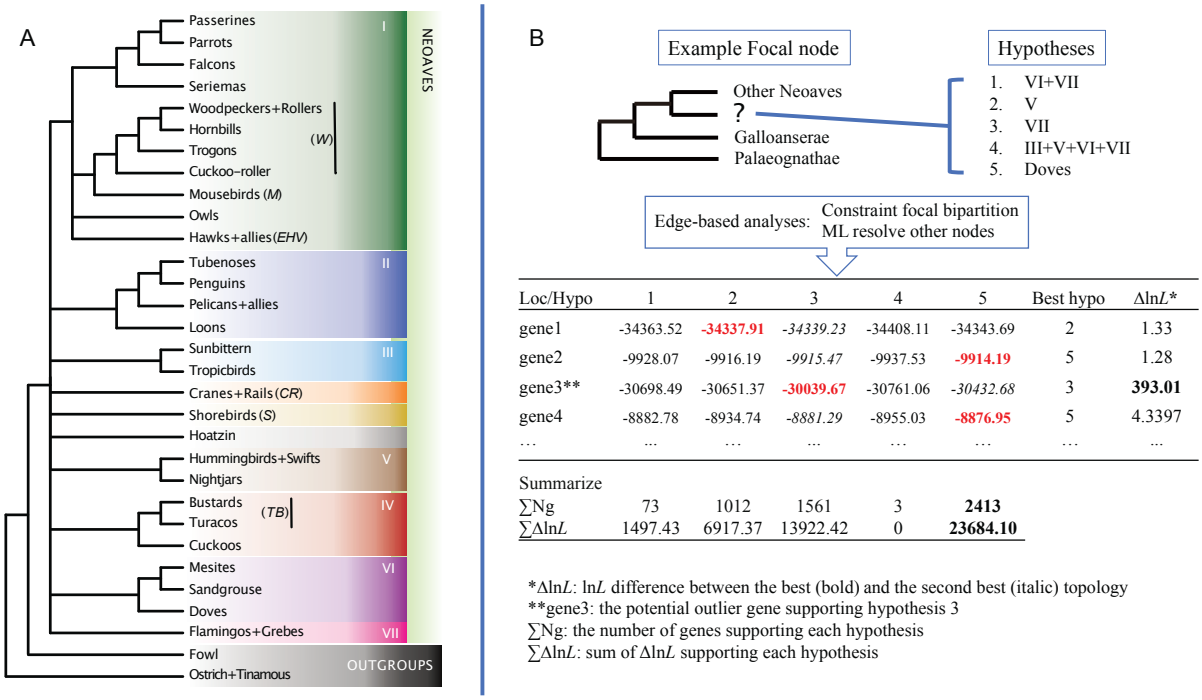

Loc/Hypo	1	2	3	4	5	Best hypo	Δln*L**
gene1	-34363.52	**-34337.91**	*-34339.23*	-34408.11	-34343.69	2	1.33
gene2	-9928.07	-9916.19	*-9915.47*	-9937.53	**-9914.19**	5	1.28
gene3**	-30698.49	-30651.37	**-30039.67**	-30761.06	*-30432.68*	3	**393.01**
gene4	-8882.78	-8934.74	*-8881.29*	-8955.03	**-8876.95**	5	4.3397
…	…	…	…	…	…	…	…
Summarize							
∑Ng	73	1012	1561	3	**2413**		
∑Δln*L*	1497.43	6917.37	13922.42	0	**23684.10**		

*Δln*L*: ln*L* difference between the best (bold) and the second best (italic) topology
**gene3: the potential outlier gene supporting hypothesis 3
∑Ng: the number of genes supporting each hypothesis
∑Δln*L*: sum of Δln*L* supporting each hypothesis

Figure 3

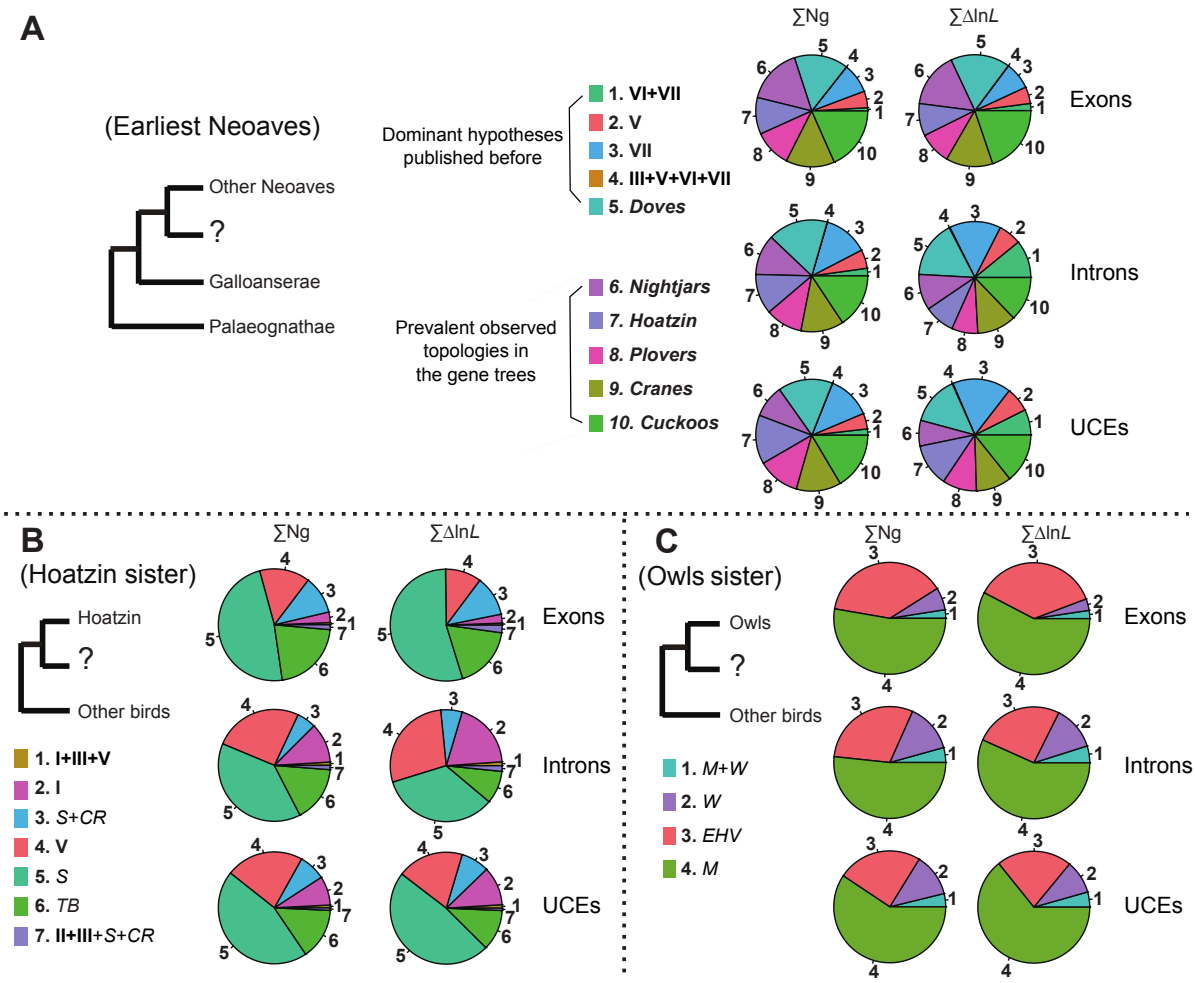
A
(Earliest Neoaves)
Other Neoaves
?
Galloanserae
Palaeognathae
Dominant hypotheses published before
1. VI+VII
2. V
3. VII
4. III+V+VI+VII
5. Doves
Prevalent observed topologies in the gene trees
6. Nightjars
7. Hoatzin
8. Plovers
9. Cranes
10. Cuckoos
∑Ng
∑ΔlnL
Exons
Introns
UCEs
B
(Hoatzin sister)
Hoatzin
?
Other birds
1. I+III+V
2. I
3. S+CR
4. V
5. S
6. TB
7. II+III+S+CR
C
(Owls sister)
Owls
?
Other birds
1. M+W
2. W
3. EHV
4. M

Figure 4

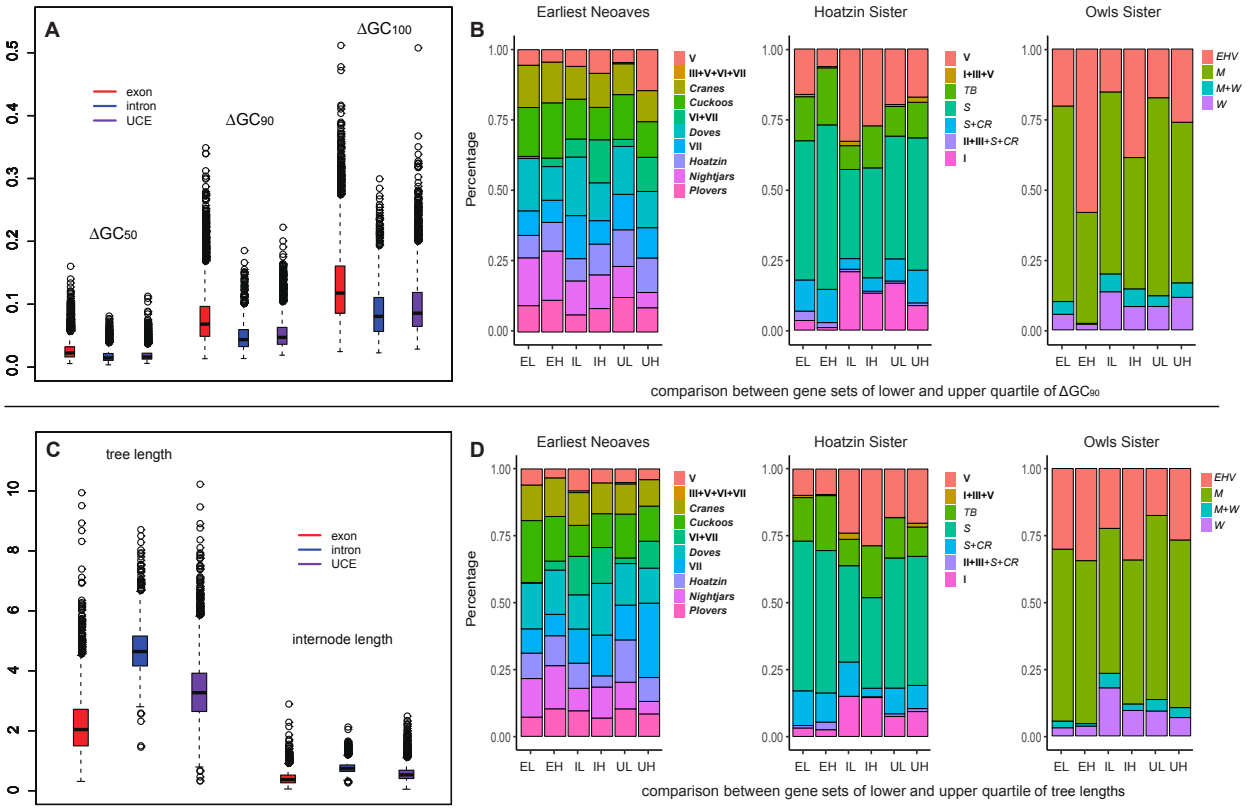
A
exon
intron
UCE
ΔGC50
ΔGC90
ΔGC100
B
Earliest Neoaves
Hoatzin Sister
Owls Sister
Percentage
V
III+V+VI+VII
Cranes
Cuckoos
VI+VII
Doves
VII
Hoatzin
Nightjars
Plovers
I+III+V
TB
S
S+CR
II+III+S+CR
I
EHV
M
M+W
W
EL EH IL IH UL UH
comparison between gene sets of lower and upper quartile of ΔGC90
C
tree length
internode length
D
comparison between gene sets of lower and upper quartile of tree lengths

Figure 5